Neutrino-nucleon scattering in the neutrino-sphere

Paulo F. Bedaque,[1,*] Sanjay Reddy,[2,†] Srimoyee Sen,[2,‡] and Neill C. Warrington[1,§]
[1]*Department of Physics, University of Maryland, College Park, Maryland 20742, USA*
[2]*Institute of Nuclear Theory, University of Washington, Seattle, Washington 98195, USA*

(Received 13 February 2018; published 31 July 2018)

We calculate the differential scattering rate for thermal neutrinos in a hot and dilute gas of interacting neutrons using linear response theory. The dynamical structure factors for density and spin fluctuations of the strongly interacting neutron matter, expected in the neutrino decoupling regions of supernovae and neutron star mergers, are calculated in the virial expansion for the first time. Correlations due to nucleon-nucleon interactions are taken into account using a pseudopotential that reproduces measured nucleon-nucleon phase shifts, and we find that attractive s-wave interactions enhance the density response and suppress the spin response of neutron matter. The net effect of neutron correlations is to strongly suppress backscattering. Moreover, we find nearly exact scaling laws for the response functions, valid for the range $T = 5$–10 MeV and $q < 30$ MeV, allowing us to obtain analytic results for the dynamic structure factors at second order in the fugacity of the neutron gas. We find that the modification of scattering rates depends on the energy and momentum exchanged. The use of dynamical structure factors can lead to corrections of the scattering rate at the 10–20% level compared to approximations based on static structure factors.

DOI: 10.1103/PhysRevC.98.015802

I. INTRODUCTION

The energy spectrum of neutrinos emerging from supernovae and neutron star mergers influences the supernova explosion mechanism, nucleosynthesis, and their detectability in terrestrial neutrino detectors. An accurate description of neutrino interactions in hot dense matter encountered in these extreme phenomena is essential to make reliable predictions for the neutrino spectrum and luminosity and has been studied extensively (see Ref. [1] for a recent review). It is known that strong interactions between nucleons and electromagnetic interactions between nucleons and charged leptons can alter neutrino scattering rates, thereby influencing the temporal and spectral features of neutrino emission from supernovae [2–7].

In this article, we shall focus on neutrino interactions in nuclear matter at moderate density ($\rho \simeq 10^{11}$–$10^{13}\,\mathrm{g/cm^3}$) and high temperature ($T = 5$–10 MeV), since these are conditions encountered in the neutrino-sphere region where neutrinos decouple from the nuclear matter and their energy spectrum is determined. Under these conditions, nucleons form a dilute gas and the fugacity of nucleons $z = e^{\mu/T}$ (where μ is the nucleon chemical potential) is a useful expansion parameter. This has been exploited to calculate the equation of state (EOS) directly in terms of the measured nucleon-nucleon phase shifts using the well-known virial expansion [8,9]. Further, since response functions in the long-wavelength limit are related to thermodynamic derivates, the virial EOS has been used to obtain neutrino scattering rates in dilute matter by neglecting corrections that depend on the energy and momentum transfer in neutrino-nucleon scattering [2,7]. The main objective of this study is to go beyond the static long-wavelength approximation used in previous studies and calculate the dynamical structure factors to assess how strong interaction corrections to the neutrino-nucleon scattering depend on the energy and momentum transfer. We shall find that dynamical structure factors alter the back-scattering rates by 10–30% for thermal neutrinos with energies in the range 10–30 MeV. Corrections of this size may be relevant for the core-collapse supernova as recent work suggests that modest variation in microphysical input can have an impact on the explosion mechanism [10–15].

II. NEUTRINO SCATTERING RATE IN A NEUTRON GAS

Although matter encountered in the neutrino-sphere contains neutrons, protons, electrons, and perhaps even small traces of light nuclei, in the following we shall focus on neutrino scattering in a pure neutron gas. This will allow us to establish the formalism and to examine in detail the effects due to nuclear interactions without the added complexity of multicomponent systems of electrons and protons, where long-range electromagnetic interactions will also need to be accounted. Further, since matter in the neutrino-sphere is close to β equilibrium, with negligibly small neutrino chemical potential, the fraction of charged particles (electrons, proton, and light nuclei) is typically much less than 10%, and neutrons dominate the scattering opacity.

*bedaque@umd.edu
†sareddy@uw.edu
‡srimoyee08@gmail.com
§ncwarrin@umd.edu

The differential scattering rate of low-energy neutrinos in a nonrelativistic gas of neutrons is given by

$$\frac{d\Gamma(E_\nu)}{d\cos\theta dq_0} = \frac{G_F^2}{4\pi^2}(E_\nu - q_0)^2\big[c_V^2(1+\cos\theta)S_V(q_0,\mathbf{q}) + c_A^2(3-\cos\theta)S_A(q_0,\mathbf{q})\big], \tag{2.1}$$

where E_ν is the energy of the incoming neutrino, q_0 is the energy transfer to the medium, and θ is the angle between the incoming and outgoing neutrino. The momentum transfer to the medium $\mathbf{q}$ is constrained by kinematics to satisfy $|\mathbf{q}| = \sqrt{4E_\nu(E_\nu - q_0)\sin^2(\theta/2) + q_0^2}$. The neutral current vector and axial vector coupling constants for the neutron are $c_V = -1/2$ and $c_A = -(g_A - \Delta S)/2$, respectively, where $g_A \approx -1.27$ and $\Delta S \approx 0$. $S_{V,A}(q_0,\mathbf{q})$ are the density and spin structure factors defined by

$$S_V(q_0,\mathbf{q}) = \int dt d^3\mathbf{r}\, e^{iq_0t - i\mathbf{q}\cdot\mathbf{r}}\langle\delta n(t,\mathbf{r})\delta n(0,0)\rangle,$$
$$S_A(q_0,\mathbf{q}) = \int dt d^3\mathbf{r}\, e^{iq_0t - i\mathbf{q}\cdot\mathbf{r}}\langle\delta \mathbf{S}(t,\mathbf{r})\delta \mathbf{S}(0,0)\rangle, \tag{2.2}$$

where the thermal average is $\langle . \rangle = \mathrm{Tr}(e^{-\beta H}.)/\,\mathrm{Tr}\, e^{-\beta H}$ and $\delta n = n - \langle n\rangle$ ($\delta\mathbf{S} = \mathbf{S} - \langle\mathbf{S}\rangle$) are the fluctuations of the density (spin). The approximations leading to Eq. (2.1) are only that the weak interaction is treated at first order in the coupling and that neutrons are nonrelativistic. The latter approximation greatly simplifies the calculation, since to order v^0 (where v is the nucleon velocity) the nucleon vector current reduces to $\bar\psi\gamma_\mu\psi \to \delta_{\mu 0}\psi^\dagger\psi$ and the axial current reduces to its spatial part $\bar\psi\gamma_\mu\gamma_5\psi \to \delta_{\mu i}\psi^\dagger\sigma_i\psi$, resulting in an expression entirely determined by the fluctuations of density and spin.

While the weak interactions between neutrinos and nucleons is perturbative, the interactions among nucleons is not, especially at the temperatures and densities encountered in the neutrino-sphere. As a consequence, methods needed to calculate the exact density and spin dynamic structure factors of a nonperturbative dense many-body system are still lacking. Perturbation theory in the strength of the strong interaction fails and nonperturbative many-body computational methods such as quantum Monte Carlo (QMC), which have been useful in obtaining ground-state energies and thermodynamic properties of strongly interacting dense Fermi systems, cannot be directly used to calculate the frequency dependence of response functions because they are formulated in imaginary time. Further, interactions between nucleons at short distances are poorly known, and three- and higher-body forces begin to play a role at and above nuclear saturation density ($\rho_{\rm sat} \approx 2.5 \times 10^{14}$ g/cm^3).

Before we calculate the dynamic structure factors and discuss the approximations involved, we present results that can be obtained with only static information about the density and spin correlation functions. By integrating over kinematically allowed energy transfers, we can rewrite Eq. (2.1) as

$$\frac{d\Gamma(E_\nu)}{dq} = \frac{G_F^2 q}{2\pi^2}\left[c_V^2\tilde S_V(q)\left(1 - \frac{q^2}{4E_\nu^2} - \frac{\omega_V}{E_\nu} + \frac{\omega_V^2}{4E_\nu^2}\right) + c_A^2\tilde S_A(q)\left(1 + \frac{q^2}{4E_\nu^2} - \frac{\omega_A}{E_\nu} - \frac{\omega_A^2}{4E_\nu^2}\right)\right], \tag{2.3}$$

where

$$\tilde S_{V/A}(q) = \int_{-q}^{\min[2E_\nu - q, q]} dq_0 S_{V/A}(q_0,q), \tag{2.4}$$

$$\omega_{V/A}^n = \frac{1}{\tilde S_{V/A}(q)}\int_{-q}^{\min[2E_\nu - q, q]} dq_0 q_0^n S_{V/A}(q_0,q). \tag{2.5}$$

Here $q = |\mathbf{q}|$ is the magnitude of the momentum transfer. The functions $\tilde S_{V/A}(q)$ are closely related to the static structure factors

$$S_{V/A}(q) = \int_{-\infty}^{\infty} dq_0 S_{V/A}(q_0,q), \tag{2.6}$$

and $\tilde S_{V/A}(q) \simeq S_{V/A}(q)$ only if a significant fraction of the response resides in the region where $-q < q_0 < \min[2E_\nu - q, q]$. For nonrelativistic and noninteracting nucleons, the characteristic energy transfer is of order $|q_0| \simeq v_{\rm th} q$, where $v_{\rm th} \simeq \sqrt{T/M}$ is the thermal velocity of nondegenerate nucleons with mass $M \gg T$. In the temperature range we are interested in ($T \simeq$ 5–10 MeV), the thermal velocity is indeed small and $\tilde S_{V/A}(q) \approx S_{V/A}(q)$ should be a good approximation. However, interactions can alter this, allowing the response to peak at larger values of $|q_0|$, and in general $\tilde S(\mathbf{q}) < S(\mathbf{q})$, implying that some dynamical information is needed to obtain a quantitative description of the scattering rates.

The integral in Eq. (2.5) that defines $\omega_{V/A}$ is closely related to the f-sum rule [16] which states that

$$\int_{-\infty}^{\infty}\frac{dq_0}{2\pi} q_0 S_{\mathcal{O}}(q_0,q) = \langle[[\mathcal{H},\mathcal{O}],\mathcal{O}]\rangle, \tag{2.7}$$

where $\mathcal{O} = \psi^\dagger\psi$ (for the density response) or $\mathcal{O} = \psi^\dagger\sigma_i\psi$ (for the spin response), and $\mathcal{H}$ is the nuclear Hamiltonian. When a large fraction of the response is kinematically accessible, the f-sum rule for the density response requires that $\omega_V = q^2/2M$, even in the presence of interactions, as a computation of the double commutator shows. Hence, we expect $\omega_V \ll E_\nu$ since typical $q \simeq E_\nu \ll M$. However, we note that since spin is not conserved by nuclear interactions, the f-sum rule for the spin response does not vanish in the long-wavelength limit [17]. One cannot guarantee that $\omega_A \ll E_\nu$ even for nonrelativistic nucleons, and calculations of the dynamical response including components of $\mathcal{H}$ that do not commute with the spin operator are needed to determine ω_A [18–20].

Nonetheless, it is common practice to adopt the elastic approximation, and in the limit ($\omega_{V/A}/E_\nu \to 0$) one obtains a simpler formula for the differential scattering rate:

$$\frac{d\Gamma(E_\nu)}{d\cos\theta} = \frac{G_F^2}{4\pi^2}E_\nu^2\big[c_V^2(1+\cos\theta)S_V(\mathbf{q}) + c_A^2(3-\cos\theta)S_A(\mathbf{q})\big], \tag{2.8}$$

which is widely used in the literature to describe neutrino-nucleon scattering at low energy [9]. Another approximation that greatly simplifies calculations is to also neglect the momentum transfer and replace $S_{V/A}(q)$ by $S_{V/A}(0)$. Since the latter is a long-wavelength property, it can be related to the equation of state [9]. The neglect of the momentum dependence is justified when the momentum transfer is small compared to the typical thermal nucleon momentum $p_{\rm thm} \simeq \sqrt{6MT}$.

For strongly correlated nucleons, other smaller momentum scales associated with correlations between particles arise and it is *a priori* unclear whether the replacement $S_{V/A}(q)$ by $S_{V/A}(0)$ is a good approximation. For these reasons, and to obtain a quantitative description of how corrections to neutrino scattering due to correlations depend on energy and momentum transfer, we calculate the dynamical structure factor.

III. METHOD

We will now discuss the calculation of the dynamical structure factors and the approximations involved. As noted earlier, the relatively low densities and high temperatures encountered in the neutrino-sphere provide a useful small expansion parameter: The fugacity of the gas defined as $z = e^{\beta\mu}$, where μ is the chemical potential and $\beta = 1/T$ is the inverse temperature. When $z \ll 1$, thermodynamic and linear response properties of gases can be obtained in the the virial expansion where observables are expressed as a power series in z. Since the fugacity is proportional to the number density at lowest order:

$$n \simeq 2\left(\frac{MT}{2\pi}\right)^{3/2} z, \tag{3.1}$$

the condition $z \lesssim 1/10$ implies that $n \lesssim 0.0005(T/5\,\text{MeV})^{3/2}\,\text{fm}^{-3}$ or $\rho \lesssim (T/5\,\text{MeV})^{3/2} 10^{12}\,\text{g/cm}^3$.

The way we treat the strong interactions involves an uncontrolled but well-motivated approximation. In the virial limit, particle-hole loops are suppressed by powers of the fugacity z, but particle-particle loops are not [21]. Since the nuclear interactions are not perturbatively small, particle-particle loops need to be summed to all orders. The calculation of all diagrams involving up to two particle-hole loops and an arbitrary number of particle-particle loops is very involved. However, if we drop all the particle-particle loops and, at the same time, substitute the interaction to have a pseudopotential vertex of the form [22]

$$V(p, p') = \frac{4\pi}{M}\left[\frac{\delta(p)}{p} + \frac{\delta(p')}{p'}\right], \tag{3.2}$$

where $\delta(p)$ is the phase shift, and p and p' are the incoming and outgoing relative momenta, one reproduces, up to order z^2, the correct thermodynamics quantities as given by the Beth-Uhlenbeck formula. Thus, for simplicity, we describe the neutron-neutron interactions by the pseudopotential, remembering to drop the particle-particle loops. This approach has the feature of including the correct, experimentally determined phase shifts, as opposed to an approximation of them. On the other hand, it is not rigorous in the sense that it is possible that the pseudopotential, despite giving exact results for static quantities, does not reproduce the exact value for nonstatic quantities.

In addition to the approximations described above, we will make the following approximations only to keep the calculations simple. First, we do not include partial waves higher than $L = 1$. This approximation is justified from the fact that at the temperatures of interest $T = 5$–10 MeV, the second virial coefficient coming from p-wave interactions between neutrons is $\sim$2 orders of magnitude less than the second virial coefficient coming from s-wave interactions. The hierarchy continues for even higher partial waves. Second, we do not include partial-wave mixing in nucleon-nucleon scattering, we neglect the contribution of protons in the medium, and we do not include the effect of charged weak currents. Third, we neglect the excitation of more than one particle from the ground state. This can be justified when the typical energy transfer $q_0 \simeq q v_{th} \gg \Gamma_n$, where Γ_n is the scattering rate of neutrons in the gas. All of these effects can be included in a straightforward manner and will be discussed in a future paper.

IV. CALCULATION

As already stated, we compute the dynamic structure factor in the virial expansion. Denoting the contribution to the structure factor $S(q_0, q)$ at nth order in the fugacity (z) expansion as $S_n(q_0, q)$, we can write

$$S(q_0, q) = S_1(q_0, q) + S_2(q_0, q) + S_3(q_0, q) + \cdots. \tag{4.1}$$

Since the structure factor should reduce to zero in vacuum, the leading nonzero contribution to it appears only in the first order in the virial expansion. As mentioned before, the number of particle-hole loops in a Feynman diagram contributing to the density-density or the spin-spin correlation identifies the lowest order in the virial expansion at which the diagram contributes [21]. This helps fix the diagrams we need to calculate at a given order in the virial expansion. To elaborate further, the first order in virial expansion includes contributions only from a single particle-hole loop, whereas the second order includes contributions from both single as well as double particle-hole loops. Since we are counting only particle-hole loops, any further reference to loops will solely imply particle-hole loops unless mentioned otherwise. We organize our calculation by splitting up the contributions coming from various loops (m) at a given order in virial expansion (n) denoted as $S_{\text{m-loop},n}$ to write

$$S_1(q_0, q) = S_{\text{1-loop},1}(q_0, q), \tag{4.2}$$

$$S_2(q_0, q) = S_{\text{1-loop},2}(q_0, q) + S_{\text{2-loop},2}(q_0, q), \tag{4.3}$$

and so on. Each of these terms are computed below for a low-density neutron gas. The neutrons are treated as a two-component spinor field in Matsubara formalism interacting via only two-body forces defined by the pseudopotential. The free neutron propagator is given by $G_{\alpha\beta}(ip_0, p) = \delta_{\alpha\beta} G(ip_0, p) = \frac{\delta_{\alpha\beta}}{ip_0 - \xi_p}$, where α, β indexes the spin. The neutron-neutron vertex is defined in Fig. 1. The phase shift $\delta(p)$ appearing in the vertex are the ${}^1S_0$ channel p-n scattering phase shifts taken from a partial-wave analysis carried out by the Theoretical High Energy Physics Group of the Radboud University, Nijmegen [23]. Our computation for the dynamic structure factor can incorporate phase shifts of any form. To compute the structure factor, we use the fluctuation-dissipation theorem [24] that relates the structure factor to the analytic continuation of the Matsubara correlation function

$$S(q_0, q) = -\frac{2}{1 - e^{-\beta q_0}} \chi(q_0, q), \tag{4.4}$$

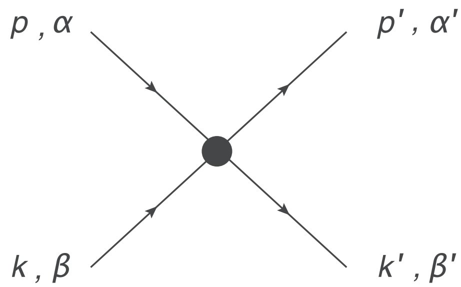

FIG. 1. The pseudopotential vertex equal to $\frac{4\pi}{M}\frac{1}{2}[\frac{\delta(\frac{|p-k|}{2})}{\frac{|p-k|}{2}} + \frac{\delta(\frac{|p'-k'|}{2})}{\frac{|p'-k'|}{2}}](\delta_{\alpha\alpha'}\delta_{\beta\beta'} - \delta_{\alpha\beta'}\delta_{\beta\alpha'})$.

where $\beta = T^{-1}$ and the susceptibility $\chi(q_0, q)$ is defined as

$$\chi(q_0, q) = \mathrm{Im}\mathcal{G}(iq_0 \to q_0 + i0^+, q). \tag{4.5}$$

Here $\mathcal{G}(iq_0, q)$ is the Fourier transform of the Mastubara time-ordered correlator $\mathcal{G}(x, \tau) = -\langle T_\tau\{\delta n(x, \tau)\delta n(0, 0)\}\rangle$.

Diagrams contributing to $\mathcal{G}(iq_0, q)$ up to $\mathcal{O}(z^2)$ are given in Figs. 2 and 3. We separate $\mathcal{G}(iq_0, q)$ into one-loop and two two-loop contributions

$$\mathcal{G}(iq_0, q) = \mathcal{G}_{\text{1-loop}}(iq_0, q) + \mathcal{G}_{\text{2-loop},\Sigma}(iq_0, q) + \mathcal{G}_{\text{2-loop},v}(iq_0, q) + \cdots . \tag{4.6}$$

We apply the same procedure to $\chi(q_0, q)$ and $S(q_0, q)$.

We start by calculating the vector structure factor $S_V(q_0, q)$ (we now drop the subscript "V" from $S_V(q_0, q)$ and related functions). The one-loop diagram gives

$$\mathcal{G}_{\text{1-loop}}(iq_0, q) = 2T\sum_{p_0}\int đ^3p\, G(p)G(p-q) = 2\int đ^3k\frac{n(\xi_{k-q/2}) - n(\xi_{k+q/2})}{iq_0 - \frac{k\cdot q}{M}}, \tag{4.7}$$

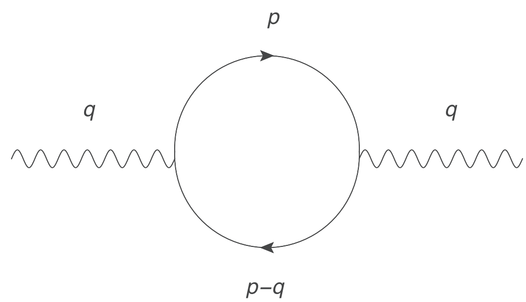

FIG. 2. Free contribution to the structure factor. This diagram contains both $\mathcal{O}(z)$ and $\mathcal{O}(z^2)$ contributions.

where $đ^3p = d^3p/(2\pi)^3$, $\xi_p = p^2/2M - \mu$, the sum runs over integer multiples of $2\pi T$ and $G(p)$ is the free neutron propagator. After using Eqs. (4.4) and (4.5), we obtain the corresponding contribution to the structure factor:

$$S_{\text{1-loop}}(q_0, q) = -\frac{2}{1 - e^{-\beta q_0}}\left[-\frac{4z}{\lambda^3 q}\sqrt{\frac{\pi M}{2T}}e^{\frac{-\beta M q_0^2}{2q^2} - \frac{\beta q^2}{8M}} \times \sinh\left(\frac{\beta q_0}{2}\right) - \left(z \to z^2 \text{ and } T \to \frac{T}{2}\right)\right] + \mathcal{O}(z^3), \tag{4.8}$$

where we have defined the de Broglie wavelength $\lambda = \sqrt{\frac{2\pi}{MT}}$. As mentioned earlier, $\mathcal{G}_{\text{1-loop}}(iq_0, q)$ contains both $\mathcal{O}(z)$ and $\mathcal{O}(z^2)$ contributions.

The expression for the two-loop self-energy diagram (left side of Fig. 3) is

$$\mathcal{G}_{\text{2-loop},\Sigma}(iq_0, q) = -4T^2\sum_{p_0,k_0}\int đ^3p\,đ^3k\,G(p)^2G(k) \times G(p-q)V(|p-k|, |p-k|). \tag{4.9}$$

After using Eqs. (4.4) and (4.5), we find the contribution of the self-energy diagram to the structure factor

$$\begin{aligned} S_{\text{2-loop},\Sigma}(q_0, q) = \frac{-z}{1 - e^{-\beta q_0}}\frac{Me^{\frac{-\beta q^2}{8MT}}}{\pi q}\Bigg(&2q_0\frac{M^2}{q^2}\sinh\left(\frac{\beta q_0}{2}\right)e^{\frac{-Mq_0^2}{2Tq^2}}\left[\Sigma\left(\sqrt{M^2q_0^2/q^2 + q^2/4 + Mq_0}\right) - (q_0 \to -q_0)\right] \\ &+ \int_{|\frac{Mq_0}{q}|}^{\infty} dkke^{\frac{-\beta k^2}{2M}}\{\beta[\Sigma(\sqrt{k^2 + q^2/4 + Mq_0})e^{-\beta q_0/2} - (q_0 \to -q_0)] \\ &+ \beta\cosh(\beta q_0/2)[\Sigma(\sqrt{k^2 + q^2/4 - Mq_0}) - (q_0 \to -q_0)] \\ &- M\sinh(\beta q_0/2)\left[\frac{\Sigma'(\sqrt{k^2 + q^2/4 - Mq_0})}{\sqrt{k^2 + q^2/4 - Mq_0}}\right] + (q_0 \to -q_0)\}\Bigg), \end{aligned} \tag{4.10}$$

where $\Sigma(p)$ is the self-energy of the neutrons given by

$$\Sigma(p) = \frac{4\pi}{M}T\sum_{k_0}\int đ^3k G(k)\frac{\delta(|p-k|/2)}{|p-k|/2} = \frac{2zT}{\pi p}\int_0^\infty dk[e^{\frac{-\beta(k-p)^2}{2M}} - e^{\frac{-\beta(k+p)^2}{2M}}]\delta(k/2) + \mathcal{O}(z^2) \tag{4.11}$$

and $\Sigma'(p) = \frac{d}{dp}\Sigma(p)$. Notice that we only need $\Sigma(p)$ computed to $\mathcal{O}(z)$ as it enters in $S_{\text{2-loop},\Sigma}(q_0, q)$ inside a particle-hole loop.

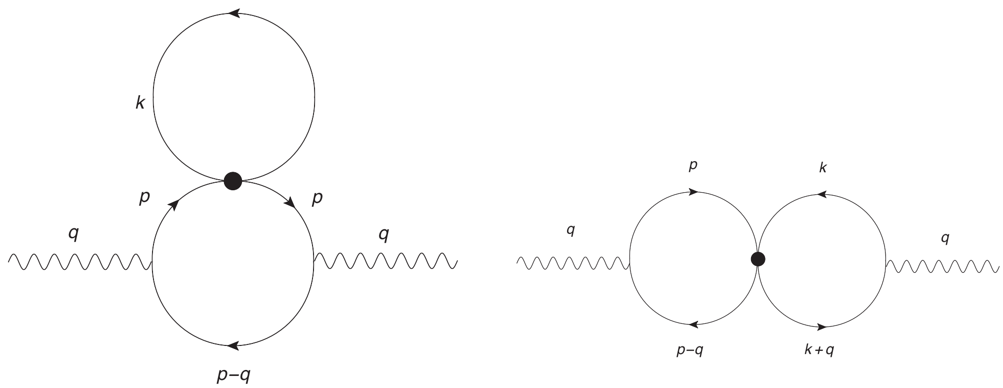

FIG. 3. Above are the $\mathcal{O}(z^2)$ contributions to the Matsubara correlation function. On the left is the self-energy correction and on the right is the vertex correction.

Finally, the diagram on the right panel of Fig. 3 gives

$$\begin{aligned}\mathcal{G}_{2\text{-loop},v}(iq_0,q) &= -2T^2\sum_{p_0,k_0}\int d\!\!{}^-{}^3p\,d\!\!{}^-{}^3k\,G(p)G(k)G(p-q)G(k+q)V(|p-k|,|p-k-2q|)\\ &= \frac{8\pi}{M}\int d\!\!{}^-{}^3k\,\frac{[n(\xi_{k+q/2})-n(\xi_{k-q/2})][n(\xi_{p+q/2})-n(\xi_{p-q/2})]}{\left(iq_0-\frac{p\cdot q}{M}\right)\left(iq_0-\frac{k\cdot q}{M}\right)}\,\frac{\delta(|k-p+q|/2)}{|k-p+q|/2}.\end{aligned} \quad (4.12)$$

Again, using Eqs. (4.4) and (4.5), we find

$$\begin{aligned}S_{2\text{-loop},v}(q_0,q) &= \frac{-2MTz^2}{1-e^{-\beta q_0}}\frac{e^{\frac{-\beta q^2}{4M}}}{q\pi^2}\int_0^\infty dk k^2 e^{-\frac{\beta k^2}{M}}\int_{-1}^1 dx\frac{M}{2kqx}\left[\frac{\delta(\sqrt{k^2+q^2/4+kqx})}{\sqrt{k^2+q^2/4+kqx}}+\frac{\delta(\sqrt{k^2+q^2/4-kqx})}{\sqrt{k^2+q^2/4-kqx}}\right]\\ &\quad\times\left(\left\{2\cosh\left[\beta\left(q_0-\frac{kqx}{M}\right)\right]e^{\frac{-\beta M}{q^2}(q_0-\frac{kqx}{M})^2}-x\to -x\right\}-\left[2\cosh\left(\frac{\beta kqx}{M}\right)e^{\frac{-\beta M}{q^2}(q_0-\frac{kqx}{M})^2}-x\to -x\right]\right).\end{aligned} \quad (4.13)$$

We conclude this section by extending these calculations to $S_A(q_0,q)$ (again, we temporarily drop the subscript "A" from $S_A(q_0,q)$ and related functions). Recall that the dynamic structure factor corresponding to spin fluctuations is given by

$$S_{ij}(q_0,q) = \int d^4x e^{iq_0t-iqx}\langle\delta s_i(x,t)\delta s_j(0,0)\rangle, \quad (4.14)$$

where the operator $\delta s_i(x,t)\equiv\psi^\dagger(x,t)\sigma_i\psi(x,t)-\langle\psi^\dagger\sigma_i\psi\rangle$ and the σ_i are the Pauli matrices. The ${}^1S_0$ interaction is spin symmetric, so clearly $\langle\delta s_i\delta s_j\rangle\sim\delta_{ij}$.

The diagrams contributing to the spin-spin correlator are of the same form as the ones in Fig. 3 except now there is an insertion of a spin operator on the vertices with a wavy line. The only consequence of this insertions is that the last (vertex correction) diagram acquires an extra minus sign compared to the density-density correlator, and thus

$$\begin{aligned}S_{A,2}(q_0,q) &= S_{1\text{-loop},2}(q_0,q)+S_{2\text{-loop},\Sigma}(q_0,q)\\ &\quad - S_{2\text{-loop},v}(q_0,q).\end{aligned} \quad (4.15)$$

The physical interpretation of Eq. (4.15) is apparent: The vertex correction contribution to the spin structure factor is suppressed due to spin antialignment in the ${}^1S_0$ channel. For attractive s-wave interactions, nucleon-nucleon correlations with antialignment spin are favored over those in which the spins are aligned. This implies that we can expect the density response to be enhanced and correspondingly the spin response to be suppressed.

The expressions in Eqs. (4.15), (4.13), (4.10), and (4.8) are our central results. They cast the calculation of the structure factors in terms of two-dimensional integrals which are computed numerically. Below we will provide very good analytic fits to these functions with few parameters.

V. SUM RULES

As a check on our calculation and to validate the use of the pseudopotential, we will show that sum rules, derived on general grounds, are indeed satisfied by our results. First, the following thermodynamic sum rule relates the vector structure factor to a thermodynamic quantity [25]:

$$\int_{-\infty}^{\infty}\frac{dq_0}{2\pi}S_V(q_0,q\to 0) = T\frac{\partial n}{\partial\mu} = \frac{2z}{\lambda^3}(1+4b_2z+\cdots), \quad (5.1)$$

where b_2 the second virial coefficient, is given by the Beth-Uhlenbeck relation [26]

$$b_2 = -\frac{1}{2^{5/2}}+\frac{\sqrt{2}}{\pi}\int_0^\infty dk\frac{d\delta(k)}{dk}e^{-\frac{\beta k^2}{M}}. \quad (5.2)$$

Here $\delta(k)$ is the phase shift of the $^1S_0$ partial wave and $k = |k_1 - k_2|/2$ is the difference in incoming momenta.

The spin structure factor satisfies a similar sum rule [9]:

$$\int_{-\infty}^{\infty} \frac{dq_0}{2\pi} S_A(q_0, q \to 0) = \frac{2z}{\lambda^3}(1 + 4b_{2,\text{free}} z + \cdots), \tag{5.3}$$

with $b_{2,\text{free}} = -2^{-5/2}$. We verified numerically that both sides of Eqs. (5.1) and (5.3) agreed for an array of parameter values and different phase shifts. In addition, our calculations were repeated in the Schwinger-Keldysh formalism, which leads to different but equivalent expressions. These expressions make it easy to see that Eq. (5.1) is satisfied exactly for any phase shift and parameter values (derived in the Appendix).

A second sum rule that can be used as a check on the calculation is the so-called *f-sum* rule [25], which was defined earlier in Eq. (2.7). Since nuclear interactions conserve baryon number, the interaction commutes with the density operator and

$$\int_{-\infty}^{\infty} \frac{dq_0}{2\pi} q_0 S_V(q_0, q) = \frac{q^2}{2M} n. \tag{5.4}$$

In addition, since we only consider s-wave interactions, the interaction also commutes with the spin operator. Consequently, the dynamic structure for spin $S_A(q_0, q)$ also satisfies the above sum rule. We numerically verified that Eq. (5.4) was satisfied for several combinations of parameter values and phase shifts. However, as noted earlier in the discussion pertaining to Eq. (2.7), the f-sum rule for the spin dynamical structure factor does not vanish in the long-wavelength limit when the Hamiltonian contains operators that do not commute with the nucleon spin operator. Such operators enhance the contribution of multiparticle excitations [17,18], and their contribution to the dynamical structure factor is necessary to satisfy the f-sum rule in Eq. (2.7). In this work, since we only include s-wave interactions, it is consistent to neglect these contributions in the long wavelength limit.

We conclude this section by estimating the range of validity for our virial expansion of the structure factor. The condition for the third and fourth terms of the virial expansion of $T\partial n/\partial\mu$ to be smaller than the second term is that

$$z < \left|\frac{4b_2}{9b_3}\right|, \left|\frac{4b_2}{16b_4}\right|^{1/2}. \tag{5.5}$$

It is not necessary to consider further higher order virial coefficients b_n since they rapidly decrease with n. The second virial coefficient for neutrons interacting in the $^1S_0$ channel is nearly constant in the temperature range $T = 5$–10 MeV and has a value $b_2 = 0.305$. We can estimate b_3 for the neutron gas as being equal to b_3 for a dilute Fermi gas in the BEC-BCS crossover region, which was computed theoretically in Ref. [27] to be temperature independent and have a value of $b_3 = -0.291(1)$. Similarly, we estimate b_4 for the neutron gas to be that of the unitary gas, which has the value $b_4 = 0.047(18)$ [13,28]. These estimates yield the condition for validity of the virial expansion to be

$$z \lesssim 0.47, 1.27. \tag{5.6}$$

Our calculations comfortably satisfy this bound. Since the static structure factor at zero momentum transfer is determined by the susceptibility $T\partial n/\partial\mu$, it is reasonable to expect that our calculation for the structure factor also lies in the range of validity of the virial expansion.

VI. SCALING FUNCTIONS AND ANALYTICAL FITS

The structure factors $S_A(q_0)$ and $S_V(q_0, q)$ can be written in terms of the functions $S_{1-\text{loop}}(q_0, q)$, $S_{2-\text{loop},\Sigma}(q_0, q)$, and $S_{2-\text{loop},V}(q_0, q)$ through the relations

$$S_V(q_0, q) = S_{\text{1-loop}}(q_0, q) + S_{\text{2-loop},\Sigma}(q_0, q) + S_{\text{2-loop},v}(q_0, q), \tag{6.1}$$

$$S_A(q_0, q) = S_{\text{1-loop}}(q_0, q) + S_{\text{2-loop},\Sigma}(q_0, q) - S_{\text{2-loop},v}(q_0, q). \tag{6.2}$$

While $S_{\text{1-loop},2}(q_0, q)$ has a very explicit form given by Eq. (4.8), the expressions for $S_{\text{2-loop},\Sigma}(q_0, q)$ and $S_{\text{2-loop},v}(q_0, q)$ involve two-dimensional integrals that need to be computed numerically. It would be useful then to have a more explicit, even if approximate, expression for these functions. To that end, we first notice that they are a function of the temperature T, the fugacity z, and the energy and momentum transfers q_0 and q. The dependence on z is, by definition, a factor of z^2. We empirically find that there is an approximate scaling relation allowing us to express $S_{\text{2-loop},\Sigma}(q_0, q)$ and $S_{\text{2-loop},v}(q_0, q)$ in terms of functions of a single variable:

$$S_{\text{2-loop},\Sigma}(q_0, q; T, z) \approx \frac{z^2}{\bar{z}^2} \frac{1 - \exp\left[-\beta q_0\left(\frac{\bar{q}}{q}\sqrt{\frac{T}{\bar{T}}}\right)\right]}{1 - \exp\left(-\beta q_0\sqrt{\frac{\bar{T}}{T}}\right)} \times S_{\text{2-loop},\Sigma}\left(q_0 \frac{\bar{q}}{q}\sqrt{\frac{\bar{T}}{T}}, \bar{q}; \bar{T}, \bar{z}\right), \tag{6.3}$$

$$S_{\text{2-loop},v}(q_0, q; T, z) \approx \frac{z^2}{\bar{z}^2} \frac{1 - \exp\left[-\beta q_0\left(\frac{\bar{q}}{q}\sqrt{\frac{T}{\bar{T}}}\right)\right]}{1 - \exp\left(-\beta q_0\sqrt{\frac{\bar{T}}{T}}\right)} \times S_{\text{2-loop},v}\left(q_0 \frac{\bar{q}}{q}\sqrt{\frac{\bar{T}}{T}}, \bar{q}; \bar{T}, \bar{z}\right), \tag{6.4}$$

where $\bar{q}$, $\bar{T}$, and $\bar{z}$ are any momentum, temperature, and fugacity reference scales. Choosing $\bar{q} = 1$ MeV, $\bar{T} = 5$ MeV, and $z = 1/4$, the functions $S_{\text{2-loop},\Sigma}(q_0, \bar{q}; \bar{T}, \bar{z})$ and $S_{\text{2-loop},v}(q_0, \bar{q}; \bar{T}, \bar{z})$ are well parametrized, in the relevant

$q = 0$–30 MeV, $T = 5$–10 MeV range of parameters by

$$S_{2\text{-loop},\Sigma}(q_0, \bar{q}; \bar{T}, \bar{z}) = A_1 e^{-|\frac{q_0}{\sigma_1}|^{2.75}}, \quad A_1 = (262.7\ \text{MeV})^2, \quad \sigma_1 = 1.252 \times 10^{-1}\ \text{MeV},$$

$$S_{2\text{-loop},v}(q_0, \bar{q}; \bar{T}, \bar{z}) = A_2 e^{-\frac{q_0^2}{\sigma_2^2}} \cos\left(\frac{q_0}{\omega}\right), \quad A_2 = (430.7\ \text{MeV})^2, \quad \sigma_2 = 8.626 \times 10^{-2}\ \text{MeV}, \quad \omega = 5.560\ \text{MeV}\cdot \tag{6.5}$$

Note that there is no restriction on z for use of the scaling law since the z dependence is known to be a factor of z^2. Figure 4 shows how well the full result compares to the scaling functions under the most extreme circumstances. Agreement only improves when the temperature or momentum transfer is decreased. Considering all the uncertainties involved in our calculation, the use of the analytic expressions in Eq. (6.6) is justified in most applications.

VII. DISCUSSION OF STRUCTURE FACTORS

In the following sections, we discuss important physical features of the dynamical structure factors we computed and the corresponding neutrino cross sections.

The most salient feature to notice in our results, generic in the relevant parameter range, is a substantial enhancement of the density-density correlation and a suppression of the spin-spin correlation. In fact, in Fig. 5 we show both the vector and axial structure factors for a free theory and the full result including $\mathcal{O}(z^2)$ correlations for parameters typically present in the neutrino-sphere ($T = 5$ MeV, $z = 1/4$, corresponding to a density of $n/n_{nuc} = 9 \times 10^{-3}$). This sizable impact of two-body correlations, even at reasonable z, can be attributed to the large neutron phase shifts. Of course, at smaller values of z, the enhancement and/or suppression is less pronounced.

The static structure factors are defined by

$$S_V(q) \equiv \int_{-\infty}^{\infty} \frac{dq_0}{2\pi} S_V(q_0, q), \quad S_A(q) \equiv \int_{-\infty}^{\infty} \frac{dq_0}{2\pi} S_A(q_0, q), \tag{7.1}$$

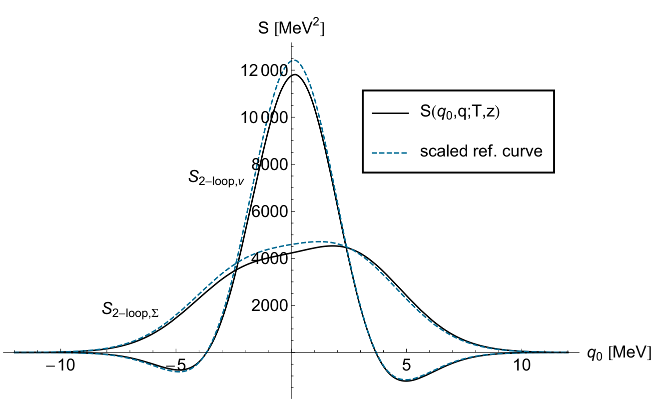

FIG. 4. In black are the exact dynamic structure factors of Eqs. (4.10) and (4.13) at $T = 10$ MeV, $z = 1/4$, and $q = 30$ MeV as a function of energy transfer. These T and q represent the upper limits of validity of our scaling law. In dashed blue is the result of applying the scaling law Eq. (6.3) to the reference curves of Eq. (6.5). The agreement between the exact structure factor and the scaling law strictly improves for lower values of T and q.

and are shown in Fig. 6. The static structure factors are a useful probe of the medium and have been up until now the only resource for computing neutrino scattering rates through Eq. (2.8). We comment on the efficacy of the static structure factor's use in computing neutrino scattering rates (as opposed to the dynamic structure factor) later on. The asymptotic behavior at large values of the momentum transfer q of both the density-density and spin-spin static structure factors approach the value of the density n, as OPE arguments demand [29]. This convergence is graphically demonstrated in Fig. 6 and is analytically demonstrated in the Appendix. At small values of the momentum transfer q, the static structure factors exhibit the same kind of enhancement (for S_V) or suppression (for S_A) as the dynamic structure factors, in line with previous observations [7].

VIII. RESULTS FOR NEUTRINO SCATTERING

The neutrino differential scattering rate is determined by the dynamic structure factors through Eq. (2.1). Since the dynamic structure factor is difficult to compute, it is customary to approximate the scattering rate by utilizing the static structure factor, which is much easier to compute, via Eq. (2.8). Now having a computation of the dynamic structure factors, we can ascertain the impact of this approximation. The comparison between the "exact" (obtained from the dynamic structure factors) and "approximate" (obtained from the static structure factors) are shown in Fig. 7. We find that the departure of

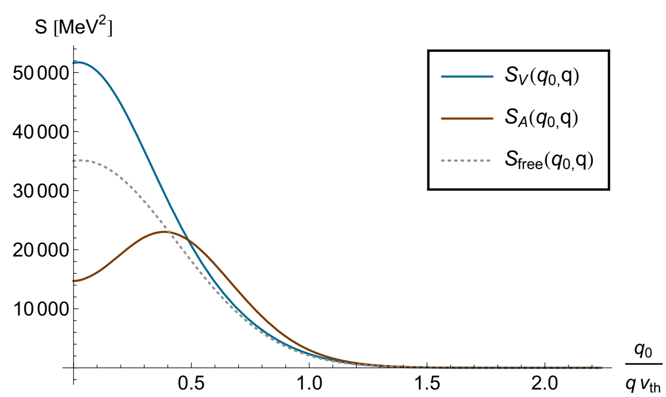

FIG. 5. Here we demonstrate the dramatic effect that neutron correlations have on the dynamic structure factor. We plot three observables: the dynamic structure factor for density correlations S_V with all contributions up to $\mathcal{O}(z^2)$ in blue, the dynamic structure factor for spin correlations S_A with all contributions up to $\mathcal{O}(z^2)$ in brown, and for comparison we have in dotted gray the free gas density structure factor to $\mathcal{O}(z)$. Here the momentum transfer is chosen to be $q = 10$ MeV and we have chosen the bulk parameters $T = 5$ MeV, $z = 1/4$ (corresponding to a density of $n/n_{nuc} = 9 \times 10^{-3}$).

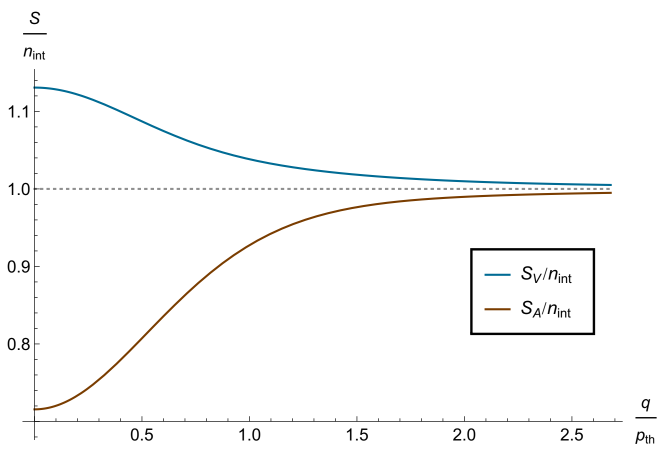

FIG. 6. Here we show the the static structure factor, computed to $\mathcal{O}(z^2)$, for density (blue) and spin (brown) at the representative temperature $T = 5$ MeV and fugacity $z = 1/4$ (corresponding to a density of $n/n_{nuc} = 9 \times 10^{-3}$). Both curves are normalized by the density computed to $\mathcal{O}(z^2)$ and we plot against the momentum scaled by the thermal momentum $p_{th} \equiv \sqrt{6MT}$. Once again it is clear that at low momenta, the density response is enhanced while the spin response is suppressed. The convergence of both static structure factors to the density is nontrivial and is predicted by the operator product expansion.

our results from the approximate result is relatively small for smaller neutrino energies (6 to 10 MeV) but is significant for higher neutrino energies around 30 MeV.

The consequences of the neutron correlations on neutrino scattering are illustrated in Fig. 8. It is found that the main effect on scattering due to neutron correlations is to strongly suppress back scattering. This can be understood by noting that neutrinos in the ultrarelativistic limit preserve their helicity and thus back scattering can only occur through their axial current coupling to the nucleon spin. However, as is demonstrated in Fig. 6, $\mathcal{O}(z^2)$ interactions suppress the spin fluctuations, and correlate nearby neutron pairs into spin singlets due to the attractive ${}^1S_0$ interactions, thereby suppressing back scattering.

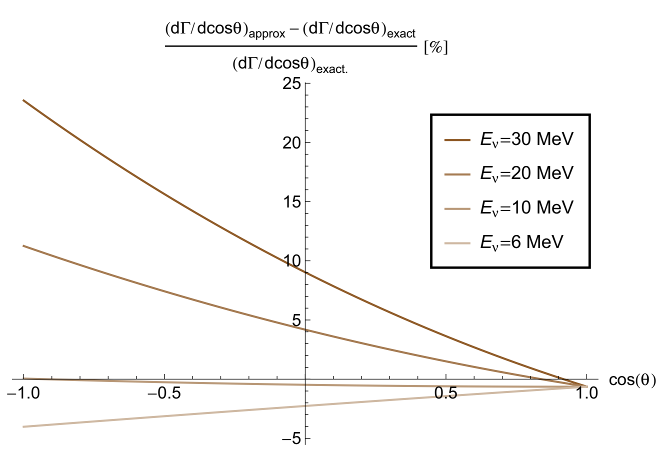

FIG. 7. To quantify the error incurred on the differential scattering rate using the static approximation Eq. (2.8), we plot the difference between the differential scattering rate calculated using the dynamic structure factor Eq. (2.1) and the static structure factor Eq. (2.8). The former is denoted as "exact" while the latter is denoted as "approx." It is seen that for neutrino energies $E_\nu < 10$ MeV, scattering rates are systematically underpredicted by no more than $\leqslant 5\%$. However, backscattering is overestimated by 10–25% for thermal neutrinos with energies in the range 15–30 MeV. The thermodynamic parameters are $T = 5$ MeV and $z = 1/4$.

In order to make it easier to use the results in Eqs. (6.5) and (6.3), it would be useful to have a simple expression relating the fugacity z to the neutron density n. Up to $\mathcal{O}(z^2)$, the relation is

$$n = \frac{2z}{\lambda^3}(1 + 2zb_2(T) + \cdots), \tag{8.1}$$

where b_2 is given by the Beth-Uhlenbeck formula in Eq. (5.2). Using the neutron-neutron s-wave phase shifts, the second virial coefficient $b_2(T)$ is well parametrized by

$$b_2(T) = a_0 + a_1 T + a_2 T^2 + \cdots \tag{8.2}$$

with

$$a_0 = 0.306, \quad a_1 = -1.17 \times 10^{-4}\ \text{MeV}^{-1},$$
$$a_2 = -1.93 \times 10^{-4}\ \text{MeV}^{-2}. \tag{8.3}$$

IX. CONCLUSION

In this work, we examined the effects of neutron interactions on neutrino scattering rates in the neutrino-sphere. Although it is difficult to analyze neutrino scattering off cold dense matter in a systematic way because of the absence of a small expansion parameter, in the high-temperature dilute gas of the neutrino-sphere the fugacity is a small parameter which can be used to make the calculations tractable. We compute the dynamic structure factor for both density and spin correlations in the virial expansion and extract from these structure factors medium modified scattering rates. Our work is meant to improve on the previous calculations of neutrino scattering in hot and dilute matter, where the scattering rates are computed in the long wavelength limit and medium effects can be expressed in terms of the equation of state. Though model independent, the long wavelength limit has its limitations because the momentum dependence of observables is completely disregarded. We compute, for the first time, the dependence of the structure factor on energy and momentum transfer from the neutrinos to the medium. We model the neutron-neutron interaction with a pseudopotential vertex in the ${}^1S_0$ channel. The pseudopotential approach takes in as input on-shell scattering phase shifts and outputs, upon calculation of Feynman diagrams, dynamical correlations. We find that upon inclusion of two-body correlations, neutrino scattering is suppressed in the medium. In particular, backscattering is most strongly suppressed. Since ${}^1S_0$ interactions between neutrons tend to anticorrelate spins into spin 0 singlets and suppress the axial response, backscattering, which can only proceed via the axial current coupling for ultrarelativistic neutrinos ($m_\nu/E \to 0$), is correspondingly suppressed. Both vector and axial currents contribute to scattering at

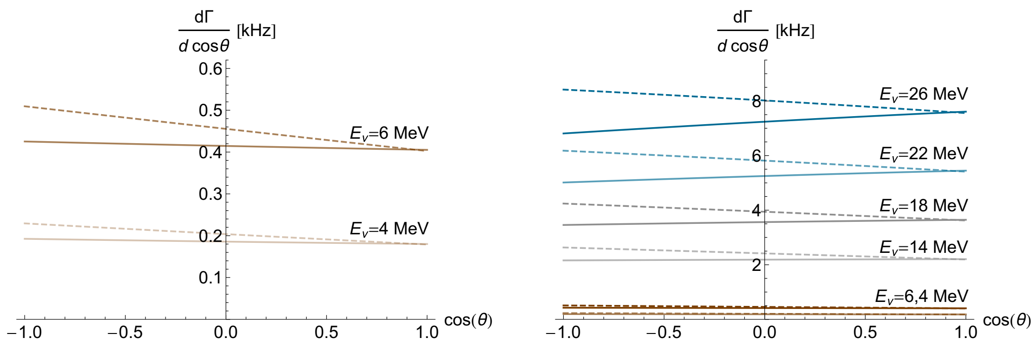

FIG. 8. Figures show the differential rate for neutrino scattering at $T = 5$ MeV and $z = 1/4$ over a range of incoming neutrino energies. The right panel is a larger view of the plot on the left, which focuses on the low-energy range. Dotted lines correspond to the $\mathcal{O}(z)$ free theory predictions, while the solid lines come from the $\mathcal{O}(z^2)$ theory.

forward angles, and the modest enhancement of the vector response partially compensates for the suppression of axial response

We have demonstrated that the pseudopotential model behaves sensibly. In particular, we have shown that the dynamic structure factor extracted from the pseudopotential approach reproduces *exactly* the thermodynamics of the neutron gas and satisfies the f-sum rule. Additionally, the pseudopotential reproduces the high-momentum predictions for the static structure factor from the operator product expansion. There are several improvements that warrant further study, and we aim to include (i) higher partial waves and (ii) two-particle excitations above the ground state in future work. In addition, to account for short-distance dynamics, two-body currents need to be included consistently. To access higher densities, the pseudopotential will need to be replaced either by realistic interactions where in the particle-particle channels are summed to higher order or by effective interactions that properly account for Pauli blocking and nucleon self-energies in the intermediate states. Although these improvements are warranted, the results presented here already mark an advance over earlier work where corrections due to strong interactions were only included in the static, long-wavelength limit.

ACKNOWLEDGMENTS

N.C.W. and P.B. are supported by U.S. Department of Energy under Contract No. DE-FG02-93ER-40762. S.R. and S.S. supported by U.S. Department of Energy under Grant Contract No. DE-FG02-00ER41132.

APPENDIX: ANALYTICAL VERIFICATION OF SUM RULES

We have used the Matsubara imaginary-time formalism for the calculations presented in the main part of this paper. In order to check some results, we repeated calculations in the Schwinger-Kelydsh real-time formalism. The real-time formalism provides mathematically equivalent, but different looking, expressions that are sometimes are easier to interpret physically. We computed $S_V(q_0, q)$ and $S_A(q_0, q)$ in both formalisms and we found exact agreement.

We presently verify the thermodynamic and high-momentum sum rules in the Schwinger-Keldyish formalism. The strength of the Schwinger-Keldysh approach is the transparency with which the sum rules are demonstrated. In the real-time formalism, every field ψ in the theory is represented by two fields ψ_+ and ψ_-. Propagators are 2×2 matrices:

$$D(p) = \begin{pmatrix} D_{++}(p) & D_{+-} \\ D_{-+}(p) & D_{--} \end{pmatrix} = \begin{pmatrix} \frac{1}{p_0-\xi_p+i0^+} + 2\pi i n(p_0)\delta(p_0-\xi_p) & 2\pi i n(p_0)\delta(p_0-\xi_p) \\ 2\pi i[n(p_0)-1]\delta(p_0-\xi_p) & -\frac{1}{p_0-\xi_p-i0^+} + 2\pi i n(p_0)\delta(p_0-\xi_p) \end{pmatrix}. \tag{A1}$$

The vertices are also doubled but remain diagonal in the $\pm$ space:

$$V_+(p) = i\frac{4\pi}{M}\left[\frac{\delta(p)}{p} + \frac{\delta(p')}{p'}\right], \quad V_-(p) = -i\frac{4\pi}{M}\left[\frac{\delta(p)}{p} + \frac{\delta(p')}{p'}\right]. \tag{A2}$$

The structure factor, in terms of the fields ψ_+, ψ_-, is given by

$$S_V(q_0, q) = \int d^4x \langle T_c\{\psi_-^\dagger(x,t)\psi_-(x,t)\psi_+^\dagger(0,0)\psi_+(0,0)\}\rangle,$$

$$S_A(q_0, q) = \int d^4x \langle T_c\{\psi_-^\dagger(x,t)\sigma_3\psi_-(x,t)\psi_+^\dagger(0,0)\sigma_3\psi_+(0,0)\}\rangle, \tag{A3}$$

where T_c is time ordering along the Schwinger-Kelydsh contour. A straightforward calculation leads to the expressions

$$S_{\text{2-loop},\Sigma}(q_0, q) = 8\pi^2 \int d\!\!^{-4}p\, \Sigma(p)\delta'(p_0-\xi_p)[n(p_0-q_0)\delta(p_0-q_0-\xi_{p-q}) + n(p_0)\delta(p_0+q_0-\xi_{p+q})] \tag{A4}$$

$$S_{\text{2-loop},v}(q_0,q)=\frac{16\pi^2z^2}{M}e^{\frac{-\beta q^2}{4M}}\int d\!\!{}^-{}^3p\,d\!\!{}^-{}^3k\;\delta(q_0-kq/M)e^{-\beta(\epsilon_p+\epsilon_k)}P\left(\frac{1}{q_0-pq/M}\right)\left(e^{-\frac{\beta(p-k)q}{2M}}-e^{\frac{\beta(p+k)q}{2M}}\right)\times V\left(\left|\frac{k-p-q}{2}\right|,\left|\frac{k-p+q}{2}\right|\right),\tag{A5}$$

where $\delta'(p_0-\xi_p)=\frac{d}{dp_0}\delta(p_0-\xi_p)$, $P(\frac{1}{x})$ denotes the principal value, $\epsilon_p=p^2/2M$, and $n(p_0)=(e^{\beta p_0}+1)^{-1}$ is the Fermi-Dirac distribution. We first demonstrate the thermodynamic sum rule, which is obtained by integrating over q_0 and then taking the $q\to 0$ limit:

$$\begin{aligned}S_{\text{2-loop},\Sigma}(q)&=\int\frac{dq_0}{2\pi}S_{\text{2-loop},\Sigma}(q_0,q)=4\pi\int d\!\!{}^-{}^4p\,\Sigma(p)\delta'(p_0-\xi_p)[n(\xi_{p-q})+n(p_0)]\\&=2z\int d\!\!{}^-{}^3p\frac{\Sigma(p)}{T}e^{-\beta\epsilon_p}+\mathcal{O}(z^3)=\frac{4z^2}{\lambda^3}\frac{\sqrt{2}}{\pi}\int_0^\infty dk e^{-\frac{\beta k^2}{M}}\frac{d\delta}{dk}+\mathcal{O}(z^3)\\&=\frac{4z^2}{\lambda^3}(b_2-b_{2,\text{free}})+\mathcal{O}(z^3).\end{aligned}\tag{A6}$$

Note that $S_{\text{2-loop},\Sigma}(q)$ is actually independent of q. Given that $S_V(q\to 0)=\partial n/\partial\mu=2\lambda^{-3}z(1+4b_2z+\cdots)$, we see that the self-energy diagram contributes a half of the thermodynamic sum rule. The remaining half comes from the vertex. To show this, integrate Eq. (A4) over frequencies:

$$S_{\text{2-loop},v}(q)=\frac{8\pi z^2}{M}e^{\frac{-\beta q^2}{4M}}\int d\!\!{}^-{}^3p\,d\!\!{}^-{}^3k e^{-\beta(\epsilon_p+\epsilon_k)}P\left(\frac{M}{(k-p)q}\right)\left[e^{-\frac{\beta(p-k)q}{2M}}-e^{\frac{\beta(p+k)q}{2M}}\right]V\left(\left|\frac{k-p-q}{2}\right|,\left|\frac{k-p+q}{2}\right|\right).\tag{A7}$$

Choosing center-of-mass coordinates $P=k+p$, $K=(k-p)/2$ and letting q approach zero, one finds

$$S_{\text{2-loop},v}(q\to 0)=-\frac{8\pi z^2}{M}\frac{2\sqrt{2}}{\lambda^3}\int d\!\!{}^-{}^3K\;e^{-\beta K^2/M}P\left(\frac{M}{Kq}\right)e^{-\frac{\beta Kq}{M}}\frac{\delta(K)}{K}.\tag{A8}$$

Utilizing the identity $\lim_{\alpha\to 0}\int_{-\alpha}^{\alpha}d\xi\,P(\frac{1}{\xi})e^{-\xi}=-2\alpha+\mathcal{O}(\alpha^2)$, one finds

$$S_{\text{2-loop},v}(q\to 0)=\frac{4z^2}{\lambda^3}\frac{\sqrt{2}}{\pi}\int_0^\infty dk e^{-\frac{\beta k^2}{M}}\frac{d\delta}{dk}=S_{\text{2-loop},\Sigma}(q\to 0).\tag{A9}$$

Thus the thermodynamic sum rule for $S_V(q)$ is verified. Moreover, from the fact that $S_{\text{2-loop},v}(q\to 0)=S_{\text{2-loop},\Sigma}(q\to 0)$, one immediately verifies the thermodynamic sum rule for the spin structure factor, $S_A(q\to 0)=2\lambda^{-3}z(1+4b_{2,\text{free}}+\cdots)$.

The asymptotic behavior of the structure factors at high momentum shown in Fig. 6 can be obtained analytically. In fact,

$$S_{\text{2-loop},v}(q\to\infty)=-\frac{8\pi z^2}{M}\frac{2\sqrt{2}}{\lambda^3}\frac{\delta(q)}{q}e^{\frac{-\beta q^2}{4M}}\int d\!\!{}^-{}^3Ke^{-\beta K^2/M}P\left(\frac{M}{Kq}\right)e^{-\frac{\beta Kq}{M}}.\tag{A10}$$

As $q\to\infty$, the angular integral converges to

$$\int_{-1}^{1}dx\,P\left(\frac{M}{Kqx}\right)e^{-\frac{\beta Kq}{M}x}\to T\frac{M^2}{K^2q^2}\left(e^{\frac{\beta Kq}{M}}-e^{-\frac{\beta Kq}{M}}\right).\tag{A11}$$

Dropping unnecessary numerical factors, one finds

$$S_{\text{2-loop},v}(q\to\infty)\propto\frac{\delta(q)}{q^3}\int dK e^{-\beta(K+q/2)^2/M}-e^{-\beta(K-q/2)^2/M}\to\frac{\delta(q)}{q^3}\sqrt{MT}\to 0.\tag{A12}$$

On the other hand, as $S_{\text{2-loop},\Sigma}(q)=4z^2\lambda^{-3}(b_2-b_{2,\text{free}})$, we see that

$$S_V(q\to\infty)=2\frac{z}{\lambda^3}(1+2b_2z+\cdots)=n,\tag{A13}$$

as depicted in Fig. 6.

[1] A. Burrows, S. Reddy, and T. A. Thompson, Nucl. Phys. A **777**, 356 (2006).

[2] R. F. Sawyer, Phys. Rev. D **11**, 2740 (1975).

[3] N. Iwamoto and C. J. Pethick, Phys. Rev. D **25**, 313 (1982).

[4] C. J. Horowitz and K. Wehrberger, Nucl. Phys. A **531**, 665 (1991).

[5] A. Burrows and R. F. Sawyer, Phys. Rev. C **58**, 554 (1998).
[6] S. Reddy, M. Prakash, J. M. Lattimer, and J. A. Pons, Phys. Rev. C **59**, 2888 (1999).
[7] C. J. Horowitz, O. L. Caballero, Z. Lin, E. O'Connor, and A. Schwenk, Phys. Rev. C **95**, 025801 (2017).
[8] C. J. Horowitz and A. Schwenk, Phys. Lett. B **638**, 153 (2006).
[9] C. J. Horowitz and A. Schwenk, Phys. Lett. B **642**, 326 (2006).
[10] T. Melson, H.-T. Janka, R. Bollig, F. Hanke, A. Marek, and B. Müller, Astrophys. J. **808**, L42 (2015).
[11] E. O'Connor, C. J. Horowitz, Z. Lin, and S. Couch, IAU Symp. **324**, 107 (2017).
[12] A. Burrows, D. Vartanyan, J. C. Dolence, M. A. Skinner, and D. Radice, Space Sci. Rev. **214**, 33 (2018).
[13] Z. Lin and C. J. Horowitz, Phys. Rev. C **96**, 055804 (2017).
[14] R. Bollig, H. T. Janka, A. Lohs, G. Martinez-Pinedo, C. J. Horowitz, and T. Melson, Phys. Rev. Lett. **119**, 242702 (2017).
[15] K. Kotake, T. Takiwaki, T. Fischer, K. Nakamura, and G. Martínez-Pinedo, Astrophys. J. **853**, 170 (2018).
[16] G. D. Mahan, *Many-Particle Physics*, 2nd ed. (Plenum, New York, 1993).
[17] E. Olsson and C. J. Pethick, Phys. Rev. C **66**, 065803 (2002).
[18] G. Raffelt and D. Seckel, Phys. Rev. D **52**, 1780 (1995).
[19] G. I. Lykasov, C. J. Pethick, and A. Schwenk, Phys. Rev. C **78**, 045803 (2008).
[20] G. Shen, S. Gandolfi, S. Reddy, and J. Carlson, Phys. Rev. C **87**, 025802 (2013).
[21] P. F. Bedaque and G. Rupak, Phys. Rev. B **67**, 174513 (2003).
[22] E. Rrapaj, J. W. Holt, A. Bartl, S. Reddy, and A. Schwenk, Phys. Rev. C **91**, 035806 (2015).
[23] http://nn-online.org.
[24] R. Kubo, Rep. Progr. Phys. **29**, 255 (1966).
[25] P. Nozieres and D. Pines, *Theory of Quantum Liquids*, Advanced Books Classics (Avalon, Boca Raton, FL, 1999).
[26] E. Beth and G. E. Uhlenbeck, Phys. (Amsterdam, Neth.) **4**, 915 (1937).
[27] X.-J. Liu, H. Hu, and P. D. Drummond, Phys. Rev. Lett. **102**, 160401 (2009).
[28] Y. Yan and D. Blume, Phys. Rev. Lett. **116**, 230401 (2016).
[29] J. Hofmann and W. Zwerger, Phys. Rev. X **7**, 011022 (2017).